

Lymphangiogenesis in Breast Cancer Correlates with Matrix Stiffness on Shear-Wave Elastography

Yoon Jin Cha^{1*}, Ji Hyun Youk^{2*}, Baek Gil Kim¹, Woo Hee Jung³, and Nam Hoon Cho¹

¹Department of Pathology, Severance Hospital, Yonsei University College of Medicine, Seoul;

Departments of ²Radiology and ³Pathology, Gangnam Severance Hospital, Yonsei University College of Medicine, Seoul, Korea.

Purpose: To correlate tumor stiffness and lymphangiogenesis in breast cancer and to find its clinical implications.

Materials and Methods: A total of 140 breast cancer patients were evaluated. Tumor stiffness was quantitatively measured by shear-wave elastography in preoperative ultrasound examination, calculated as mean elasticity value (kPa). Slides of resected breast cancer specimens were reviewed for most fibrotic area associated with tumor. D2-40 immunohistochemical staining was applied for fibrotic areas to detect the lymphatic spaces. Microlymphatic density, tumor stiffness, and clinicopathologic data were analyzed.

Results: Higher elasticity value was associated with invasive size of tumor, microlymphatic density, histologic grade 3, absence of extensive intraductal component, presence of axillary lymph node metastasis, and Ki-67 labeling index (LI) in univariate regression analysis, and associated with Ki-67 LI and axillary lymph node metastasis in multivariate regression analysis. Microlymphatic density was associated histologic grade 3, mean elasticity value, and Ki-67 LI in univariate regression analysis. In multivariate regression analysis, microlymphatic density was correlated with mean elasticity value.

Conclusion: In breast cancer, tumor stiffness correlates with lymphangiogenesis and poor prognostic factors.

Key Words: Breast neoplasms, lymphangiogenesis, fibrosis, elasticity imaging techniques

INTRODUCTION

Fibrosis of tumors contributes to invasion and progression thereof.¹ As a tumor grows, intratumoral hypoxia is induced, and the hypoxia-inducible factor (HIF)-1 α pathway is activated. Concomitantly, abnormally activated tumor fibroblasts activate vascular endothelial growth factor (VEGF), which induces (lymph)angiogenesis.² Hypoxia also induces Wnt/beta-catenin signaling. Studies have demonstrated that activated beta-catenin is associated with metastatic potential and poor

prognosis in several cancers.^{3,4} In breast cancer, tumor fibrosis has been shown as a surrogate marker for hypoxia and (lymph) angiogenesis.^{5,6} Fibrotic tumor stroma induces angiogenesis by promoting the expression of hypoxia-related genes, resulting in tumor progression and metastasis via lymphovascular invasion.^{7,8}

Screening breast ultrasound (US) plays an important role in detection of early breast cancer.⁹ Recently, shear-wave elastography (SWE) has been used to evaluate breast mass stiffness during routine US examination since the method helps to differentiate benign from malignant masses.^{10,11} As the elasticity value reflects the hardness of an object and has been found to correlate with fibrosis, SWE is also used to screen for prostate cancer^{12,13} and evaluate for liver fibrosis in patients with hepatitis and primary biliary cirrhosis.¹⁴ Moreover, as SWE takes great advantage of quantitative estimation, statistical analyses of the correlation between various histologic parameters and tumor stiffness are possible. Studies investigating the association between a higher elasticity value and higher rate of prediction of cancer diagnosis have been reported.¹⁵⁻¹⁷ In this study, we aimed to correlate lymphangiogenesis with the stiffness of

Received: April 23, 2015 **Revised:** August 3, 2015

Accepted: September 1, 2015

Corresponding author: Dr. Nam Hoon Cho, Department of Pathology, Severance Hospital, Yonsei University College of Medicine, 50-1 Yonsei-ro, Seodaemun-gu, Seoul 03722, Korea.

Tel: 82-2-2228-1767, Fax: 82-2-362-0860, E-mail: cho1988@yuhs.ac

*Yoon Jin Cha and Ji Hyun Youk contributed equally to this work.

•The authors have no financial conflicts of interest.

© Copyright: Yonsei University College of Medicine 2016

This is an Open Access article distributed under the terms of the Creative Commons Attribution Non-Commercial License (<http://creativecommons.org/licenses/by-nc/3.0>) which permits unrestricted non-commercial use, distribution, and reproduction in any medium, provided the original work is properly cited.

breast cancers and to analyze the value of predicting lymph node metastasis and other clinicopathologic parameters.

MATERIALS AND METHODS

Patients and clinicopathologic data

This study has been approved by the Institutional Review Board of Severance Hospital (IRB No. 4-2015-0113). Between July 2012 and March 2013, 639 breast masses were imaged by gray-scale US and SWE. Core needle biopsy demonstrated breast cancer in 150 patients, who subsequently underwent mastectomy with axillary lymph node dissection. After excluding 10 patients who had received neoadjuvant chemotherapy, data from 140 patients were analyzed in this study. Pathology reports of the preoperative biopsy and mastectomy specimens were reviewed and hematoxylin and eosin slides of resected specimen were reviewed to determine the histologic type, invasive size, extensive intraductal component (EIC, defined as occu-

pying 25% or more of the tumor area), histologic grade, lymphovascular invasion, and axillary lymph node metastasis.

SWE examinations

Breast US examinations were performed using the Aixplorer US system (SuperSonic Imagine, Aix-en-Provence, France), which was equipped with a 4–15-MHz linear-array transducer, by one of four radiologists with 5–10 years of experience in breast US exams. The investigators were aware of the clinical examination and mammography results at the time of examination. After obtaining gray-scale US, SWE images were obtained for breast masses that were scheduled for biopsy or surgical excision. The built-in region-of-interest (ROI) (Q-box; SuperSonic Imagine) of the system was set to include the lesion and surrounding normal tissue, which was displayed as a gray-scale image overlaid with a semitransparent color map of tissue stiffness, ranging from dark blue, which indicated the lowest stiffness, to red, which indicated the highest stiffness (0–180 kPa). Areas of black on the SWE images represented tissue in which no shear wave

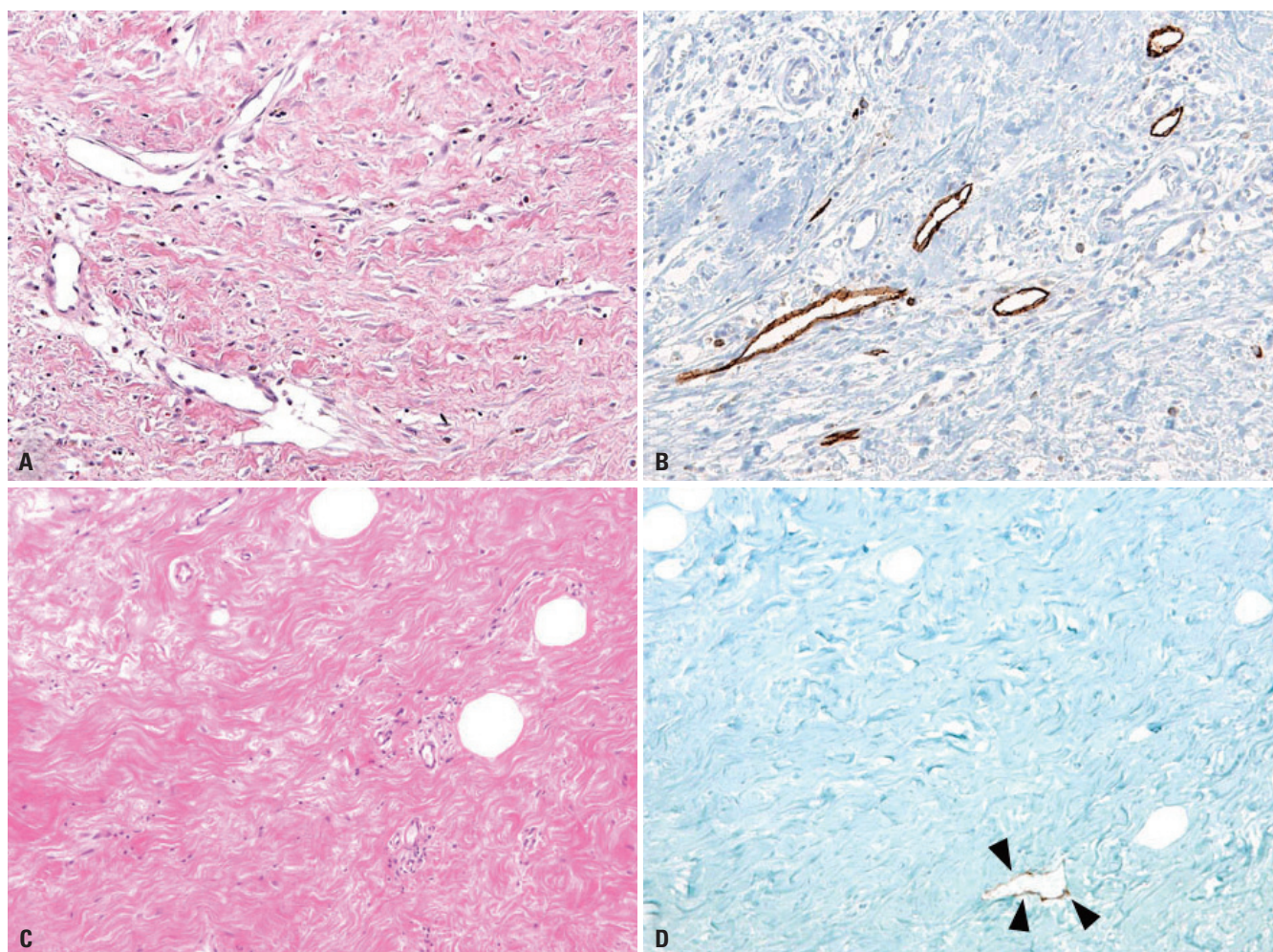


Fig. 1. Lymphangiogenesis in fibrous stroma in tumor with high elasticity value and low elasticity value. In tumor with high elasticity value (case 19, mean elasticity value: 230.0 kPa) shows lymphatic spaces (maximal microlymphatic density: 23.0) embedded in fibrotic tumor stroma (A), which are highlighted by D2-40 immunohistochemical staining (B). In tumor with low elasticity value (case 116, mean elasticity value: 56.5 kPa), lymphatic space is rarely found in fibrotic area (C) by D2-40 staining (D) (arrowheads).

was detected. Fixed 2×2-mm ROIs were placed by an investigator over the stiffest part of the lesion, including immediate adjacent stiff tissue or halo. The system calculated the mean elasticity values in kPa for the mass.

Interpretation of immunohistochemistry and HER2 fluorescence *in situ* hybridization evaluation

For the immunohistochemical evaluation of ER, PR, HER2, and Ki-67 labeling index (LI) status, formalin-fixed, paraffin-embedded (FFPE) tissue sections obtained from the surgical specimens were stained with appropriate antibodies for ER (clone 6F11; 1:200; Novocastra, Newcastle upon Tyne, UK), PR (clone 16; 1:200; Novocastra), Ki-67 (clone MIB-1; 1:1000; Dako, Glostrup, Denmark), HER2 (clone 4B5; prediluted; Roche diagnostics). A cut-off value of ≥1% positively stained nuclei was used to define ER and PR positivity.⁹ HER2 staining was analyzed

according to the American Society of Clinical Oncology/College of American Pathologists guidelines, using the following categories: 0=no immunostaining; 1+=weak incomplete membranous staining in <10% of the tumor cells; 2+=complete membranous staining, either uniform or weak, in ≥10% of the tumor cells; and 3+=uniform intense membranous staining in ≥30% of the tumor cells.¹⁸ HER2 immunostaining was considered positive when strong (3+) membranous staining was observed, whereas 0 or 1+ cases were considered negative. Tumors with a score of 2+ were sent for fluorescence *in situ* hybridization (FISH) testing performed using the PathVysion HER2 DNA Probe Kit (Abbott-Vysis, Des Plaines, IL, USA). This test determines the HER2 amplification in the event the ratio of the HER2 gene signal to chromosome 17 signal is more than 2, which is classified as positive.

Based on immunohistochemistry or FISH results of ER, PR,

Table 1. Results from Univariate Regression Analysis of Clinicopathological Variables and the Mean Elasticity Value

Variable	Number (total=140)	Mean elasticity value (kPa)	β coefficient	p value
Age			-0.122±0.376	0.745
Size of invasive tumor			12.49±3.84	0.001
Maximal microlymphatic density			1.106±0.496	0.027
Histologic type				
Ductal	111	142.52±52.26	6.84±11.98	0.569
Lobular	7	151.74±39.17	16.07±22.28	0.472
Specified	22	135.68±49.47	0	
Molecular type				
Luminal A	64	135.89±40.12	0	
Luminal B	18	151.57±70.60	15.67±13.68	0.254
HER2	32	143.56±56.02	7.66±11.10	0.491
TNBC	26	147.97±54.48	12.07±11.93	0.313
Histologic grade				
1	29	122.25±48.80	0	
2	78	140.56±51.95	18.31±10.80	0.092
3	33	162.35±44.38	40.10±12.63	0.002
Extensive intraductal component	38	126.14±47.70	-21.45±9.57	0.027
Axillary lymph node metastasis	40	165.23±57.47	32.65±9.18	0.001
Lymphovascular invasion	18	161.94±62.23	22.99±12.79	0.075
ER				
Negative	42	147.82±55.52	0	
Positive	98	139.37±49.13	-8.45±9.43	0.371
PR				
Negative	60	146.53±54.76	0	
Positive	80	138.43±48.19	-8.10±8.73	0.355
HER2				
Negative	108	141.41±49.79	0	
Positive	32	143.56±56.02	2.14±10.62	0.836
p53				
Negative	72	139.50±49.72	0	
Positive	68	144.44±52.73	4.94±8.66	0.569
Ki-67 labeling index			0.857±0.28	0.003

TNBC, triple-negative breast cancer.

HER2, and Ki-67 LI status, the tumors were divided into four subtypes: luminal A (ER-positive and/or PR-positive, HER2-negative, and Ki-67 LI<14%); luminal B (ER-positive and/or PR-positive, HER2-negative, and Ki-67 LI ≥14% or ER-positive and/or PR-positive and HER2-positive, irrespective of Ki-67 LI); HER2-enriched (ER-negative, PR-negative, and HER2-positive); and triple-negative breast cancer (TNBC) (ER-negative, PR-negative, and HER2-negative).

Microlymphatic density

To evaluate lymphangiogenesis, available 134 FFPE tissue sections obtained from the surgical specimens were stained with antibodies against D2-40 (1:100; Dako). Immunohistochemical staining for D2-40 was performed on the most fibrotic area around the tumor (Fig. 1). Each stained slide was examined at 100× magnification and counted for lymphatic spaces. Completely

D2-40 surrounded spaces without containing red blood cells were counted.

Statistical analysis

The mean elasticity value (calculated using SWE) and microlymphatic density were correlated with clinicopathologic parameters using univariate and multivariate regression models. Data were analyzed using the statistical software SPSS (version 20, SPSS Inc., Chicago, IL, USA). Differences with *p*<0.05 were considered statistically significant.

RESULTS

The mean age of the 140 patients included in this study was 52.7 years (range 28–81 years). The mean elasticity value was

Table 2. Results from Univariate Regression Analysis of Clinicopathological Variables for Lymphangiogenesis in Breast Cancer

Variable	Number (total=134)	Maximal microlymphatic density	β coefficient	p value
Age			-0.09±0.07	0.154
Size of invasive area			0.78±0.69	0.258
Mean elasticity value			0.033±0.015	0.027
Histologic type				
Ductal	107	13.93±9.05	1.49±2.14	0.490
Lobular	7	9.43±6.24	-3.02±3.86	0.435
Specified	20	12.45±7.98	0	
Molecular type				
Luminal A	61	12.21±6.49	0	
Luminal B	18	13.94±12.30	1.73±2.36	0.465
HER2	30	14.67±9.09	2.45±1.97	0.214
TNBC	25	14.80±10.41	2.59±2.09	0.219
Histologic grade				
1	26	11.62±6.55	0	
2	76	12.95±9.35	1.33±1.98	0.502
3	32	16.25±8.61	4.64±2.30	0.046
Extensive intraductal component	38	14.74±9.74	1.76±1.69	0.299
Axillary lymph node metastasis	39	15.03±10.18	2.18±1.67	0.193
Lymphovascular invasion	18	16.78±12.93	3.81±2.21	0.087
ER				
Negative	41	15.22±10.14	0	
Positive	93	12.71±8.07	-2.51±1.64	0.128
PR				
Negative	59	14.10±9.15	0	
Positive	75	12.99±8.54	-1.12±1.53	0.468
HER2				
Negative	104	13.13±8.72	0	
Positive	30	14.67±9.09	1.53±1.83	0.403
p53				
Negative	68	12.15±7.44	0	
Positive	66	14.85±9.87	2.70±1.51	0.075
Ki-67 labeling index			0.11±0.05	0.030

TNBC, triple-negative breast cancer.

141.90 kPa (range 16.10–294.30 kPa). The mean of maximal number of lymphatic spaces was 13.48 (range 1–53). The histological cancer types were as follows: invasive ductal carcinoma (n=111, 79.3%), invasive lobular carcinoma (n=7, 5.0%), and others (n=22, 15.7%; four medullary, four tubular, three mucinous, two micropapillary, two papillary, two pleomorphic, two cribriform, one apocrine, one metaplastic, and one solid papillary). Based on immunohistochemistry or FISH results of ER, PR, HER2, and Ki-67 LI status, the molecular cancer types were as follows: luminal A (n=64, 45.7%), luminal B (n=18, 12.9%), HER2 (n=32, 22.9%), and TNBC (n=26, 18.6%).

By univariate regression analysis, mean elasticity value was positively correlated with the invasive tumor size, histologic grade 3, Ki-67 LI, axillary lymph node metastasis, and microlymphatic density, and negatively correlated with EIC (Table 1). No significant differences were found among histologic or molecular types of tumor. Lymphovascular invasion showed tendency of correlation with the mean elasticity value. Microlymphatic density was associated significantly with mean elasticity value, histologic grade 3, and Ki-67 LI (Table 2). By multivariate regression analysis, axillary lymph node metastasis ($p=0.03$) and Ki-67 LI ($p=0.045$) were significantly correlated with mean elasticity value (Table 3). In terms of lymphangiogenesis, significant correlation was observed between mean elasticity value and maximal microlymphatic density ($p=0.044$) (Table 4). However, histologic grade, axillary lymph node metastasis, EIC, and Ki-67 LI did not correlate with maximal microlymphatic density.

DISCUSSION

In this study, we aimed to correlate tumor stiffness, measured by SWE, with clinicopathologic parameters and lymphangiogenesis of breast cancer. As shown in the previous studies, large invasive size, axillary lymph node involvement, higher histologic grade, increased proliferative index, lymphovascular invasion were significantly correlated with higher elasticity value.

Table 3. Results from Multivariate Regression Analysis of Clinicopathologic Variables and the Mean Elasticity Value

Variable	β coefficient	<i>p</i> value
Ki-67 labeling index	0.57±0.28	0.045
Axillary lymph node metastasis	28.0±9.16	0.003
Maximal microlymphatic density	0.84±0.48	0.085
Extensive intraductal component	-16.15±9.31	0.085

Table 4. Results from Multivariate Regression Analysis of Clinicopathologic Variables for Lymphangiogenesis in Breast Cancer

Variable	β coefficient	<i>p</i> value
Mean elasticity value	0.03±0.02	0.044
Ki-67 labeling index	0.10±0.05	0.058
Extensive intraductal component	2.91±1.68	0.085

ue.^{10,11,19,20} However, the EIC showed a negative correlation with the mean elasticity value in our study. This might be due to the lack of a desmoplastic reaction in intraductal component, in contrast to the invasive tumor which induces desmoplastic fibrosis and higher elasticity value. Also, there was no significant correlation between histologic and molecular subtypes with tumor thickness. According to Chang, et al.,¹⁰ tumor elasticity varied significantly based on histologic subtypes. Contrastingly, Youk, et al.¹⁹ reported no significant correlation between tumor elasticity and histologic and molecular subtypes. These contradictory results indicate the requirement for further precise investigation into whether histologic and molecular subtypes correlate with tumor stiffness.

Multivariate regression analysis demonstrated that axillary lymph node metastasis was independently associated with high elasticity value, which was consistent with an earlier study that reported high elasticity value as an independent predictive factor of axillary lymph node metastasis.²¹ Also, studies have also shown that a higher histologic grade, large invasive size, and histologic subtypes of TNBC and HER2 types correlate independently with a higher elasticity value.^{10,11,19} However, in this study, only axillary lymph node metastasis was independently correlated with high elasticity value, which may be attributed to our relatively small sample size. In a prior study, Youk, et al.¹⁹ showed that Ki-67 LI in tumor cells correlated with higher elasticity value in univariate regression analysis, while multivariate analysis showed only a tendency towards correlation. However, our data showed a significant association between Ki-67 LI and elasticity value. This discordance might originate from different methods of data analysis used in the two studies: we analyzed Ki-67 LI as a continuous variable, whereas Youk, et al.¹⁹ divided patients into two groups according to Ki-67 LI, namely Ki-67>14% and Ki-67≤14%.

Lymphangiogenesis was found to be strongly associated with higher elasticity value, histologic grade, and Ki-67 LI in univariate regression analysis. Higher histologic grade and Ki-67 LI are frequently observed in malignant tumors, which are associated with poor prognosis,²² which exhibit rapid progression, frequent metastasis, and (lymph)angiogenesis.^{23,24} However, axillary lymph node metastasis was not found to be correlated with lymphangiogenesis in univariate and multivariate regression analyses in present study. Only the mean elasticity value was independently correlated with lymphangiogenesis. This result suggests that tumor stiffness is important for developing new lymphatic spaces, which is consistent with prior studies in the literature demonstrating an association between tumor fibroblast and hypoxia with (lymph)angiogenesis.^{5,25} Apart from metastasis, Lee, et al.¹⁸ reported that breast cancer patients having multiple primary cancers show poor prognosis, although the breast cancer was at an early stage. It would be worthy to analyze the elasticity value of patients with multiple primary cancers and correlate the elasticity value and clinicopathologic characteristics of those patients.

Fibrosis observed in the center and periphery of tumors correlates well with elasticity value. In malignant tumors, the extracellular matrix (ECM) induces abnormal crosslinking of collagen, which could explain the higher elasticity value observed in malignant tumors. ECM-induced activation of the phosphoinositide 3-kinase pathway is thought to play an important role in tumor cell invasion.²⁴ Fibrotic foci in cancer have also been shown to be associated with poor prognosis, as well as lymphangiogenesis and angiogenesis.^{1,5,26}

Unlike normal fibroblasts in the wound healing process, tumor fibroblasts are continuously activated. VEGF is critical in the development of this reactive stroma in tumors. Additionally, intratumoral hypoxia induces activation of the HIF-1 α pathway, and VEGF induces angiogenesis.⁷ More angiogenesis is induced as the fibrotic area of the tumor expands, which could be the result of interaction between the tumor stroma and intratumoral hypoxia.²⁵ In addition, expression of carbonic anhydrase IX, a hypoxia marker, has been found to be associated with tumor fibrosis.²⁷ In previous studies, HIF-1 α and VEGF induce lymphangiogenesis and angiogenesis, that these two hypoxia-related molecules are thought to be linked to tumor aggressiveness and poor prognosis.^{6,28}

In this study, we confirmed that mean elasticity value correlated significantly with poor prognostic factors. Additionally, we found that tumor stiffness was independently correlated with lymphangiogenesis. Our data also suggest that tumor stiffness measured by SWE may be related to hypoxia-related gene expression and activation of cancer fibroblasts, which could be potential targets by therapeutic strategies for treating cancer. In conclusion, lymphangiogenesis in breast cancer correlated significantly with the mean elasticity value, which reflects tumor stiffness and poor prognosis.

ACKNOWLEDGEMENTS

This research was supported by the Basic Science Research Program through the National Research Foundation of Korea (NRF) funded by the Mid-career Researcher Program by the MEST (No. 2012R1A2A4A01006435; CNH).

REFERENCES

- Kalluri R, Zeisberg M. Fibroblasts in cancer. *Nat Rev Cancer* 2006;6:392-401.
- Fukumura D, Xavier R, Sugiura T, Chen Y, Park EC, Lu N, et al. Tumor induction of VEGF promoter activity in stromal cells. *Cell* 1998;94:715-25.
- Liu L, Zhu XD, Wang WQ, Shen Y, Qin Y, Ren ZG, et al. Activation of beta-catenin by hypoxia in hepatocellular carcinoma contributes to enhanced metastatic potential and poor prognosis. *Clin Cancer Res* 2010;16:2740-50.
- Zhang Q, Bai X, Chen W, Ma T, Hu Q, Liang C, et al. Wnt/ β -catenin signaling enhances hypoxia-induced epithelial-mesenchymal transition in hepatocellular carcinoma via crosstalk with hif-1 α signaling. *Carcinogenesis* 2013;34:962-73.
- Van den Eynden GG, Colpaert CG, Couvelard A, Pezzella F, Dirix LY, Vermeulen PB, et al. A fibrotic focus is a prognostic factor and a surrogate marker for hypoxia and (lymph)angiogenesis in breast cancer: review of the literature and proposal on the criteria of evaluation. *Histopathology* 2007;51:440-51.
- Van der Auwera I, Van den Eynden GG, Colpaert CG, Van Laere SJ, van Dam P, Van Marck EA, et al. Tumor lymphangiogenesis in inflammatory breast carcinoma: a histomorphometric study. *Clin Cancer Res* 2005;11:7637-42.
- Harris AL. Hypoxia--a key regulatory factor in tumour growth. *Nat Rev Cancer* 2002;2:38-47.
- Vaupel P. The role of hypoxia-induced factors in tumor progression. *Oncologist* 2004;9 Suppl 5:10-7.
- Hwang JY, Han BK, Ko EY, Shin JH, Hahn SY, Nam MY. Screening ultrasound in women with negative mammography: outcome analysis. *Yonsei Med J* 2015;56:1352-8.
- Chang JM, Park IA, Lee SH, Kim WH, Bae MS, Koo HR, et al. Stiffness of tumours measured by shear-wave elastography correlated with subtypes of breast cancer. *Eur Radiol* 2013;23:2450-8.
- Evans A, Whelehan P, Thomson K, McLean D, Brauer K, Purdie C, et al. Invasive breast cancer: relationship between shear-wave elastographic findings and histologic prognostic factors. *Radiology* 2012;263:673-7.
- Pallwein L, Aigner F, Faschingbauer R, Pallwein E, Pinggera G, Bartsch G, et al. Prostate cancer diagnosis: value of real-time elastography. *Abdom Imaging* 2008;33:729-35.
- Pozzi E, Mantica G, Gastaldi C, Berardinelli M, Choussos D, Bianchi CM, et al. The role of the elastography in the diagnosis of prostate cancer: a retrospective study on 460 patients. *Arch Ital Urol Androl* 2012;84:151-4.
- Corpechot C, Carrat F, Poujol-Robert A, Gaouar F, Wendum D, Chazouillères O, et al. Noninvasive elastography-based assessment of liver fibrosis progression and prognosis in primary biliary cirrhosis. *Hepatology* 2012;56:198-208.
- Roca B, Resino E, Torres V, Herrero E, Penades M. Interobserver discrepancy in liver fibrosis using transient elastography. *J Viral Hepat* 2012;19:711-5.
- Van der Auwera I, Cao Y, Tille JC, Pepper MS, Jackson DG, Fox SB, et al. First international consensus on the methodology of lymphangiogenesis quantification in solid human tumours. *Br J Cancer* 2006;95:1611-25.
- Jitsuiki Y, Hasebe T, Tsuda H, Imoto S, Tsubono Y, Sasaki S, et al. Optimizing microvessel counts according to tumor zone in invasive ductal carcinoma of the breast. *Mod Pathol* 1999;12:492-8.
- Lee J, Park S, Kim S, Kim J, Ryu J, Park HS, et al. Characteristics and survival of breast cancer patients with multiple synchronous or metachronous primary cancers. *Yonsei Med J* 2015;56:1213-20.
- Youk JH, Gweon HM, Son EJ, Kim JA, Jeong J. Shear-wave elastography of invasive breast cancer: correlation between quantitative mean elasticity value and immunohistochemical profile. *Breast Cancer Res Treat* 2013;138:119-26.
- Choi WJ, Kim HH, Cha JH, Shin HJ, Kim H, Chae EY, et al. Predicting prognostic factors of breast cancer using shear wave elastography. *Ultrasound Med Biol* 2014;40:269-74.
- Evans A, Rauchhaus P, Whelehan P, Thomson K, Purdie CA, Jordan LB, et al. Does shear wave ultrasound independently predict axillary lymph node metastasis in women with invasive breast cancer? *Breast Cancer Res Treat* 2014;143:153-7.
- Inwald EC, Klinkhammer-Schalke M, Hofstädter F, Zeman F, Koller M, Gerstenhauer M, et al. Ki-67 is a prognostic parameter in breast cancer patients: results of a large population-based cohort of a cancer registry. *Breast Cancer Res Treat* 2013;139:539-52.
- Butcher DT, Alliston T, Weaver VM. A tense situation: forcing tu-

- mour progression. *Nat Rev Cancer* 2009;9:108-22.
24. Levental KR, Yu H, Kass L, Lakins JN, Egeblad M, Erler JT, et al. Matrix crosslinking forces tumor progression by enhancing integrin signaling. *Cell* 2009;139:891-906.
 25. Colpaert C, Vermeulen P, van Beest P, Goovaerts G, Weyler J, Van Dam P, et al. Intratumoral hypoxia resulting in the presence of a fibrotic focus is an independent predictor of early distant relapse in lymph node-negative breast cancer patients. *Histopathology* 2001; 39:416-25.
 26. Kornegoor R, Verschuur-Maes AH, Buerger H, Hogenes MC, de Bruin PC, Oudejans JJ, et al. Fibrotic focus and hypoxia in male breast cancer. *Mod Pathol* 2012;25:1397-404.
 27. Colpaert CG, Vermeulen PB, Fox SB, Harris AL, Dirix LY, Van Marck EA. The presence of a fibrotic focus in invasive breast carcinoma correlates with the expression of carbonic anhydrase IX and is a marker of hypoxia and poor prognosis. *Breast Cancer Res Treat* 2003;81:137-47.
 28. Van den Eynden GG, Smid M, Van Laere SJ, Colpaert CG, Van der Auwera I, Bich TX, et al. Gene expression profiles associated with the presence of a fibrotic focus and the growth pattern in lymph node-negative breast cancer. *Clin Cancer Res* 2008;14:2944-52.